Paramagnetic Meissner effect in high-temperature superconductors: Experiments and interpretation

Yusheng He,* C. M. Muirhead, and W. F. Vinen
School of Physics and Space Research, University of Birmingham, Birmingham B15 2TT, United Kingdom
(Received 27 July 1995; revised manuscript received 12 January 1996)

The results are presented of experiments on the paramagnetic Meissner effect, the appearance of a net paramagnetic moment when some high-temperature superconductors (especially Bi-Sr-Ca-Cu-O) are cooled in a very small magnetic field. For ease of interpretation the experiments relate exclusively to Bi-Sr-Ca-Cu-O in finely powdered form. Attention is paid not only to the magnetic moment observed during a field cool, but also to the moment remaining during a subsequent zero-field warm and to the moment developed during a field warm following a zero-field cool. The moments observed during a field cool are similar to those reported by other authors. A tentative interpretation of the results is made in terms of a model in which there is a concentration within the material of small local moments that can be polarized during a field cool. Information about both the magnitudes of these local moments and their concentrations is deduced. Evidence is presented that the observed local moments are too small to be accounted for by half flux quanta trapped in loops or within grains, such half flux quanta being associated with π junctions or d-wave pairing. This suggests that either the local moments originate in some other way or the model is incorrect.

I. INTRODUCTION

All high-temperature superconductors (HTS's) are type II in their magnetic behavior. Generally, they exhibit irreversible magnetic behavior, consistent with that expected from the trapping of flux lines, although reversible behavior can be observed at high temperatures, where the flux lines are sufficiently mobile for equilibrium flux distributions to be achieved within the time scale of an experiment. The HTS material can be in various forms: a bulk single crystal; bulk material consisting of large numbers of small grains that are coupled together through weak superconducting links, as is the case with the common sintered granular form of the material; or powder in which there is no superconducting contact between grains. In the sintered granular form of the material, the network of weak links behaves in many ways like a conventional type-II superconductor, with a penetration depth that depends on the strength of the weak links.[1] A conventional type-II superconductor is as a rule diamagnetic, in the sense that, when it is cooled through its transition temperature T_c in a fixed external magnetic field, flux is expelled, although the amount of flux expelled may be small if the material is magnetically irreversible.

However, some HTS materials, when cooled in a sufficiently small magnetic field, acquire a net *paramagnetic* moment. This paramagnetic moment seems to be superimposed on a conventional Meissner diamagnetism and on any conventional trapped flux, and the moment is found to be frozen in if the external field is removed at a low temperature. The effect was reported by Svedlindh *et al.*,[2] who interpreted it in terms of a Kosterlitz-Thouless transition coupled with flux trapping. There were early concerns that the effect might be instrumental,[3] but an extensive amount of work on a range of samples in a variety of cryostats has shown that this cannot be the case. Spurious effects due to paramagnetic impurities have also been ruled out on the grounds that no significant paramagnetism is observed in the normal state in a large field (up to 0.8 T) (Ref. 4) and that the onset of paramagnetism always occurs a few degrees below T_c even when T_c is changed by 20 K by altering the oxygen concentration.[5] The effect is therefore well established and is now known as the *paramagnetic Meissner effect* (PME) or the *Wohlleben effect*.

Most of the reported work has been on the 2212 phase of Bi-Sr-Ca-Cu-O in melt-processed,[4–7] sintered,[2,7,8] and powdered[5,9,10] form, although the PME has also been seen in the 2223 phase,[4,5,10] in an erbium compound,[11] and in single crystals of Y-Ba-Cu-O.[12–14]

A paramagnetic moment could arise in an assembly of loops (with or without weak links) over certain ranges of field if the loops are noninteracting and all of essentially the same size (this moment is closely related to the Little-Parks effect). However, in the limit of very small applied fields the moment is always diamagnetic, and a range of loop sizes will also lead to a net diamagnetism, which disappears at high fields. Otherwise, it is tempting to suggest that the effect must arise from the breaking somewhere in the system of time-reversal symmetry, and it is for this reason that the effect is of great potential interest. However, it has also been suggested by a number of authors recently[15–17] that in disk-shaped specimens a paramagnetic moment can arise from conventional flux trapping, although this suggestion has not yet been explored for the case of very small particles with which this paper is concerned.

A very simple superconducting system that does break time-reversal symmetry is a superconducting loop containing one (or more generally an odd number of) Josephson junctions in which the coupling energy is negative (a π junction).[18] Provided that the McCumber parameter (β; see Sec. IV A) is sufficiently large, the state of lowest energy of such a loop in zero applied magnetic field is doubly degenerate, with a trapped flux equal to approximately $\pm\phi_0/2$. A

π junction can arise in a weak link between a conventional and a suitable unconventional superconductor[19,20] and also in weak links in which electron spin flips can occur in the barrier region.[18,21,22] More significantly perhaps in the present context, effective π junctions can form between two differently oriented crystals of a d-wave superconductor,[23] a fact that is important in the interpretation of recent observations of the trapping of half flux quanta in Y-Ba-Cu-O tricrystals as providing evidence for d-state pairing in that material.[24,25]

The idea that samples of HTS's exhibiting the PME incorporate for some reason an array of loops containing π junctions has been suggested in a number of papers. The paramagnetic moment then arises from a polarization of the loops in the applied magnetic field. The loops have been regarded either as isolated from one another[23] or as interacting with each other magnetically.[26,27] The observed magnetization in an applied field H has been fitted empirically to a relation of the form[4,5,7,8,10]

$$M=\chi_0 H+\frac{M_0 H}{H+H_0}, \tag{1.1}$$

where M_0 and H_0 are constants. The negative term $\chi_0 H$ is a conventional diamagnetic (Meissner) contribution to the moment, and it may also include the effect of flux trapping. The second term on the right-hand side of (1.1) describes the PME, it being suggested that the parameter H_0 arises from an antiferromagnetic ordering of the loop moments in an ''orbital glass'' state.[4,5,26,27] Some treatments have concentrated on the value of the ''crossover field'' H_{c0} at which the observed magnetization vanishes. It has been suggested, albeit on the basis of very simple and unrealistic models,[23,26] that this field is related to the area S of the average loop through the relation

$$H_{c0}=\frac{\phi_0}{q\mu_0 S}, \tag{1.2}$$

where the numerical factor q is either 2 or 4, depending on the exact model. Loop diameters of order 5 μm were derived in Ref. 8 in this way. Numerical simulations based on loop models and giving some agreement with experiment were described in Ref. 28. Account was taken of a distribution of critical currents at the junctions, of a reasonable assumed temperature dependence of these critical currents, and of the possibility of thermally excited jumping between quantum states of the loops. Numerical simulations based on a two-dimensional orbital glass model were described in Refs. 29,30.

The appearance of the PME in some samples correlates with the observation of anomalies in the dependence of ac and microwave response on a steady applied magnetic field.[4,5,7,31,32] For example, in powdered samples showing no PME the microwave absorption has a minimum at zero applied field, whereas in samples that do show the PME the microwave absorption exhibits a *maximum* at zero field, with minima when the applied field is of order ± 0.1 mT. Khomskii[33] has reviewed many of these experiments and their theoretical interpretation.

This paper has two aims. First, we present new experimental results on a range of finely powdered Bi-Sr-Ca-Cu-O samples exhibiting the PME, the results relating not only to the paramagnetic moment observed during cooling in an applied field (a ''field cool''), but also to the remanent moment and its temperature dependence, observed after removal of the field at various temperatures (for example, during a ''zero-field warm''). Second, we offer a different approach to the interpretation of the experimental results. We shall argue that the form of the PME suggests that it can be accounted for in terms of a *local moment model*: i.e., that it is due to an assembly of a fixed number of entities that acquire permanent magnetic moments when the sample is cooled through the superconducting transition temperature, these moments becoming partially aligned under the influence of an external magnetic field, but we make no assumption initially about the nature of the entities. By suitable analysis of the experimental results, including the observations on remanent moments, we can deduce both the density of these entities in each sample and a distribution of magnetic moments. An assumption in this analysis that magnetic interactions between the entities can be neglected is justified by the results. Trapping of conventional flux lines is also seen in our *finely powdered* samples, but we argue that it is small in the smallest magnetic fields and that it seems to occur independently of the PME. (This argument would not hold for less finely powdered samples or for sintered samples.) The magnetic moments associated with the entities turn out to be smaller than can reasonably be explained in terms of half flux quanta. We deduce that half flux quanta are not involved and that some other explanation of the PME must be invoked.

II. EXPERIMENTAL METHOD

A. Specimens

Almost all the experimental results that we report relate to finely powdered samples produced commercially by spray pyrolosis, either as received or after some processing. A few results obtained on sintered material and on powder produced by crushing bulk material will be mentioned towards the end of the paper. In the spray pyrolosis process, a nitride solution with the appropriate cation ratio is forced under pressure through a nozzle into a furnace, the resulting powder being calcined and annealed. For the most part we used the 2212 phase with a T_c of 80–83 K. Scanning electron microscope studies of this powder, as received, showed it to consist of clumps, predominantly with diameters of about 5, 20, and 50 μm. These clumps were in turn made up from much smaller platelets of irregular size and shape but typically about 2 μm$\times$2 μm$\times$0.2 μm, randomly oriented, with the c axis normal to the plane of the platelet. Careful inspection of many larger platelets showed them to consist of smaller platelets, closely adhered together. Although the platelets within a clump appear to touch at their edges, with a contact area of order 0.2–0.4 μm^2, it is not immediately clear whether or not they are in electrical or superconducting contact. Typical scanning electron microscope (SEM) photographs are shown in Fig. 1. One of our samples (NRA) was of the 2223 phase with a T_c of 108 K, again obtained by spray pyrolosis, but with a small addition of lead to stabilize

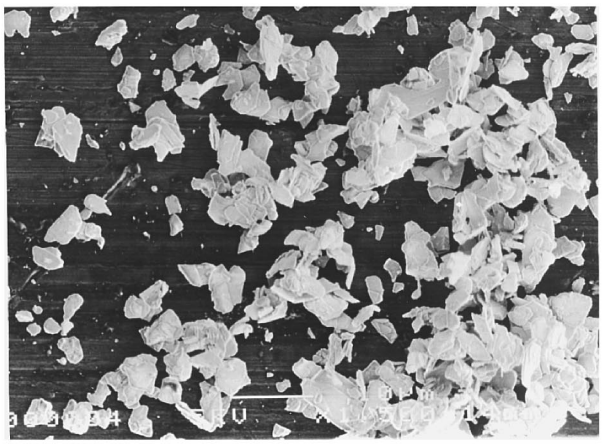

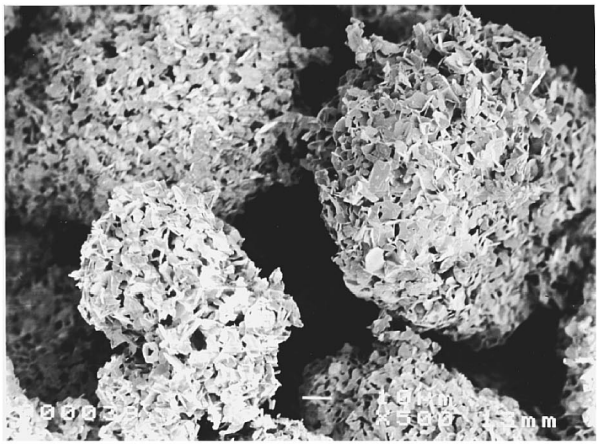

FIG. 1. Scanning electron micrographs of two samples. (a) Fine powder having a typical clump size of 3–8 μm (sample MPA); (b) a coarser powder having a typical clump size of 20—100 μm (sample MLB).

it. In some cases, powder specimens with a narrow range of clump sizes were obtained by sedimentation in a column of dry acetone.

The samples for which detailed data are presented later in the paper were as follows. Samples MRA, MRB, and MRC, obtained by spray pyrolosis, were unselected as to particle size and in the band 0–100 μm. Other samples obtained by spray pyrolosis were particle size selected: MLA and MLB in the band 20–100 μm; MPA-1,2,3 and MPB-1,2,3 in the band 3–8 μm; and MSA in the band less than 3 μm.

Some of these powders were subjected to further thermal and mechanical treatment. The sample MPA-2 is simply MPA-1 remeasured after it had been taken to room temperature for 1 week. MPA-3 was obtained by first sealing MPA-2 under argon in a glass ampoule and then cycling it 300 times between room temperature and 77 K over a period of 3 months. MPB-2 was obtained from MPB-1 by first sealing it under air in a glass ampoule, which was then placed under water in a conventional ultrasonic bath for 4 h. MPB-3 was obtained from MPB-2 by compressing it in a brass die under a pressure of 10^{10} N m^{-2}.

For the magnetic measurements described below, each powder sample was encased in 100-μm-thick aluminum foil. A hole of cross section 1.4×1.6 mm^2 and depth 3.0 mm in a brass block was lined with the foil and the powder pushed gently into the hole. The foil was folded over the top, the resulting aluminum box containing the powder removed from the hole, trimmed, and sealed all over with a thinned layer of GE7031 varnish. The structure of the randomly oriented platelets might be expected to yield a packing fraction of about 0.1. However, the insertion of the powder into the aluminum container involves some compression (albeit small), and we find that our observed packing fractions are around 0.2. Each complete sample contained around 2×10^{14} platelets per kilogram. In our various calculations we have taken the density of bulk Bi-Sr-Ca-Cu-O to be 6.5×10^3 kg m^{-3}.

B. Magnetic measurements

Measurements at low magnetic field were performed with a home-made superconducting quantum interference device (SQUID) magnetometer, very similar to one described earlier.[34] The superconducting pickup coil is in the form of a first-order gradiometer, with the sample held stationary in one half, and is connected to the input coil of a low-noise commercial dc SQUID. The sample temperature could be controlled between 4.2 and 120 K. A magnetic field up to 0.5 mT could be applied with a small solenoid surrounding the sample without driving an unacceptably large current through the SQUID input coil, the field homogeneity over the sample being about 2%. The whole assembly was enclosed by a thin lead tube at 4.2 K and a μ-metal shield at room temperature. Separate measurements with a flux gate magnetometer showed that, after cooling through the transition temperature of the lead shield, the residual field trapped at the position of the sample was less than 50 nT. The vertical component of this field could be reduced to less than 10 nT by passing a current through the solenoid and using the signal from the sample on cooling through its critical temperature as a sensor of any residual field. All electrical leads were carefully filtered against rf interference, and the control and measurement electronics were mounted well away from the cryostat. Measurements were normally taken either during heating at a rate of 100 mK s^{-1} or during cooling at a rate of 30 mK s^{-1}. This rate was chosen for two reasons: to ensure that a negligible temperature difference existed between the sample and the thermometer, and to avoid a dependence of the sample signal on cooling rate, as explained later.

High-field (0.1–10 mT) measurements were made in a commercial SQUID magnetometer (Cryogenic Consultants Ltd., model S100) which has a residual field of about 5 μT and which takes measurements by moving the sample slowly up and down within the coils of a second-order superconducting gradiometer. The magnetic field was homogeneous to within 2% along the 30-mm measurement scan.

III. EXPERIMENTAL RESULTS

In presenting the observed magnetic behavior we shall, for the sake of clarity, first present schematic diagrams, examples of actual experimental data being presented later.

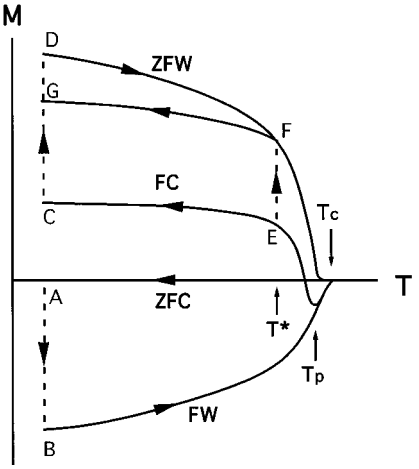

FIG. 2. Schematic diagram illustrating the temperature dependence of the magnetic moments of our samples under various warming and cooling conditions.

Schematically, the behavior is summarized in Figs. 2 and 3; Fig. 2 relates to a sample showing a strong paramagnetic Meissner effect, in the case when the magnetic field H, when applied, is small. The way in which the behavior is changed when H is changed is shown in Fig. 3. This behavior is very similar to that observed by other authors.

The field-warm (FW) line ($B \rightarrow T_c$) is obtained by first cooling the specimen in zero field ($T_c \rightarrow A$), then applying a field H ($A \rightarrow B$), and then warming in this constant field. The field-cool (FC) line ($T_c \rightarrow E \rightarrow C$) is obtained by cooling in the constant field H. The zero-field-warm (ZFW) line ($D \rightarrow F \rightarrow T_c$) is obtained by first performing a field cool, then removing the field ($C \rightarrow D$), and then warming in zero field. As we see from Fig. 3, the FC line is paramagnetic along most of its length only at fields below a crossover field H_{c0}.

We find that the observed magnetic moments along the

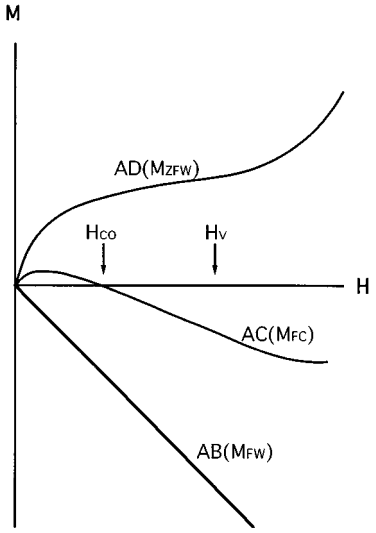

FIG. 3. Schematic diagram illustrating the field dependence of the magnetic moments of our samples under various warming and cooling conditions.

ZFW, FC, and FW curves satisfy the equation

$$M_{\mathrm{ZFW}} = M_{\mathrm{FC}} - M_{\mathrm{FW}} \tag{3.1}$$

within experimental error, at least for the data discussed in this paper (i.e., for the full range of fields at low temperatures and for low fields for the full range of temperatures up to T_c). It may be true more generally. The FC line is reversible provided that temperature changes are made sufficiently slowly; if cooling takes place too quickly (greater than about 200 mK s^{-1}), the paramagnetism is reduced. Included in Fig. 2 is the result of removing the applied field during a field cool at a relatively high temperature T^* (say, 70 K): $E \rightarrow F$. Immediately after the field removal, there is some relaxation, the moment tending to fall over time by typically 10–20 %. The decay is such that the change in moment is proportional to the logarithm of the time. The amount by which the moment relaxes over a given time decreases with decreasing temperature, and relaxation practically disappears when T^* is less than about 50 K. The ZFW line is not reversible, except at the lowest temperatures (20 K or less): if the sample is warmed from D to F and then cooled, it follows the line FG. The line FG is the same whether the point F is reached by a ZFW or by field removal from the point E. When the specimens are subjected to mechanical stress, mechanical damage, or thermal cycling, the ZFW line moves towards the T axis and the FC line moves towards the FW line, provided that the applied field is less than a value H_v ($\mu_0 H_v \sim 0.5$–1.0 mT), which also marks a change in behavior of M_{ZFW} and M_{FC}, as shown in Fig. 3. For fields $H \gg H_v$, the moment M_{ZFW} is found empirically to obey an equation of the form

$$M_{\mathrm{ZFW}} = aH^{\alpha}, \tag{3.2}$$

where the exponent α is typically about 1.6. We note that the PME sets in only at a temperature below T_p, which is itself about 2–3 K below T_c. Along the line AB in Fig. 3 the moment M_{FW} is proportional to H and reversible, provided that the temperature is less than about 50 K and the field less than 2–4 mT. This fact is consistent with flux being excluded from a fixed proportion of the sample when a field is applied after a zero-field cool, by straightforward diamagnetic screening currents without flux line penetration; however, the corresponding ''diamagnetic fraction'' (defined as the ratio of the observed magnetic moment in field B to that expected for complete flux exclusion in a bulk sample with the same total mass and *zero demagnetizing coefficient*) turns out to vary from sample to sample, to be typically in the range 0.2–0.5, and not to vary in any systematic way with clump size. If the field application $A \rightarrow B$ is carried out at a temperature above about 50 K, the measured moment M_{FW} is no longer either strictly reversible or accurately proportional to H and can no longer be due entirely to simple diamagnetic screening.

Examples of actual experimental data are shown in Figs. 4–11.

IV. INTERPRETATION OF THE EXPERIMENTAL RESULTS

Analysis of our experimental data in terms of the local moment model (which is described in detail in Sec. IV C)

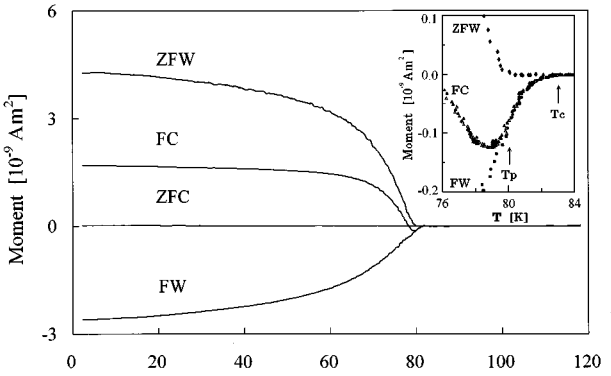

FIG. 4. Magnetic moment plotted against temperature for sample MRA under FW, FC, and ZFW conditions. The magnitude of the applied field $\mu_0 H$ is 10 μT, at which there is little flux trapping. The inset shows the region close to T_c in more detail and includes the temperature T_p above which there is no significant PME. The magnitude of T_p is almost completely independent of $\mu_0 H$ for our powder samples over the range 0.2–100 μT. This is in contrast to the behavior of our bulk samples where T_p falls by 1–2 K as the field is increased to 200 μT. This latter effect is probably associated with conventional flux trapping, T_p then being an irreversibility temperature.

must take account of the fact that they may be affected by trapping of conventional flux lines. Such trapping might be associated with supercurrents that are either *intergranular* or *intragranular*. Our use of fine unsintered powders serves to minimize these types of flux trapping and facilitates the subsequent theoretical analysis. We first analyze our field-warm data and conclude that the observed diamagnetic fractions are explicable in terms of diamagnetic screening within individual platelets, any intergranular screening currents being negligible (Sec. IV A). It follows that there can be no significant amount of *intergranular* flux trapping. From further

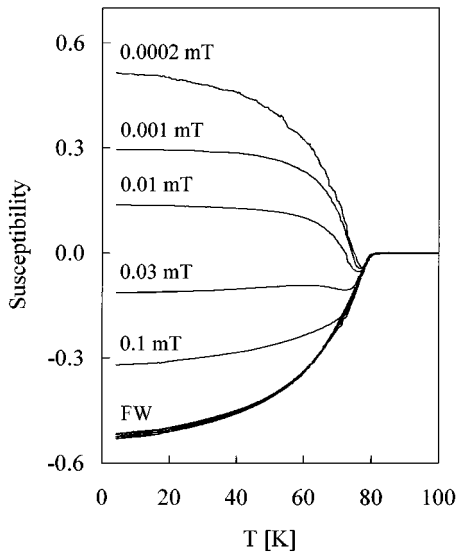

FIG. 5. FC and FW susceptibilities plotted against temperature for sample MPA-1. These results are similar to those reported by other authors. The susceptibility is defined as the ratio of the magnetic moment per unit volume of the (fully compressed) material to the applied magnetic field.

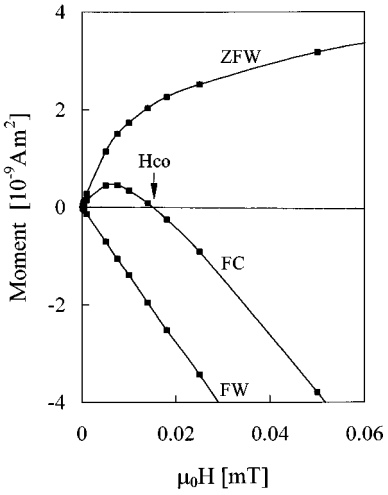

FIG. 6. ZFW, FC, and FW magnetic moments for sample MLB plotted against applied field for a temperature of 30 K. The FW line is reversible at this temperature.

analysis of our field-warm and field-cool data, we argue that, although significant *intragranular* flux line trapping can occur, it is small at low magnetic fields and can be allowed for (Sec. IV B). Suitably corrected values of M_{ZFW} can then be taken as direct measures of the PME. We show that the behavior of this deduced PME is consistent with the predictions of the local moment model (Sec. IV D), but that the magnitude of the majority of the local moments is much smaller than would be expected from half flux quanta in loops that violate time-reversal symmetry (Sec. IV E). Finally, we comment briefly on the behavior of bulk samples and compare our approach with analyses based on orbital glass models (Sec. IV F).

A. Diamagnetic fractions

We noted in Sec. III that after a zero-field cool to a low temperature the application of a small magnetic field to our

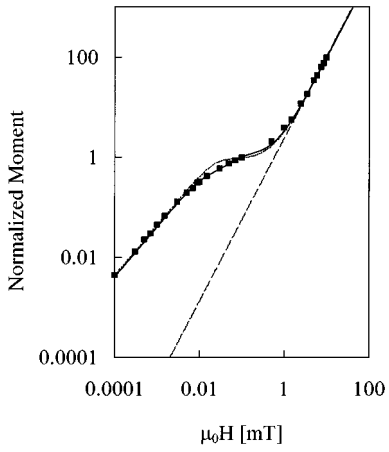

FIG. 7. ZFW magnetic moment of sample MSA at 10 K plotted against applied field (the moment is normalized to its value at an applied field of 0.1 mT). The rise at the highest fields tends to the $H^{1.6}$ power law, associated with flux trapping in the powdered samples. The dotted line is the best fit with a single-tanh function; the solid line to a double-tanh function. The dashed line is a fit of the high-field data to Eq. (3.2).

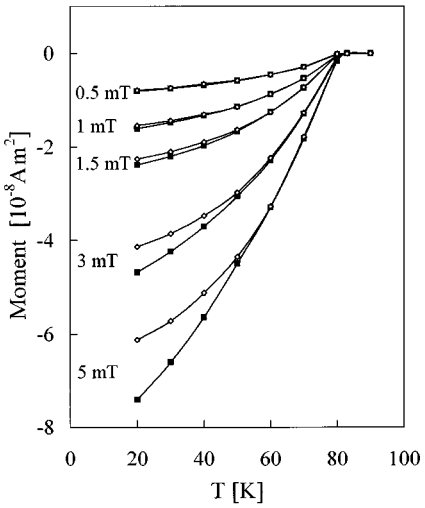

FIG. 8. FC(◇) and FW (■) magnetic moments plotted against temperature for various applied fields for the heavily crushed sample MPB-3, which shows no apparent PME and a Meissner fraction of only 0.044. Note that for fields below about 0.5 mT the two moments are equal within the accuracy of the S100 magnetometer, but that they differ by an increasing amount as the field is increased, the difference being due to conventional flux trapping.

powdered samples led to a reversible diamagnetic moment M_{FW}, due to diamagnetic screening, with a ''diamagnetic fraction'' in the range 0.2–0.5.

We recall that the powdered samples consist of clumps of platelets and that, *a priori*, the platelets within a clump may

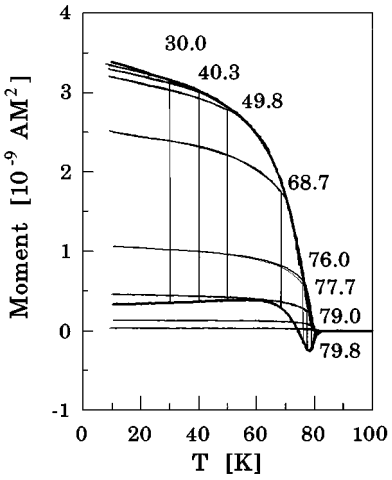

FIG. 9. FC and ZFW magnetic moments plotted against temperature for sample MRB. The sample is first cooled in a field of 10 μT (lower heavy line) to a temperature T^* (eight different values are shown), and the applied field is then reduced to zero. The sample is left for 3–4 min, during which there is a rapid flux creep, and it is then cooled at the usual rate to 10 K. Subsequent warming follows the same path up to T^*, above which the path joins the normal ZFW curve (upper heavy line). Traversing the full ZFW curve normally takes about 10 min. A small step at T^* is seen in some of the data. This arises because the amount of flux creep that occurs during the 3–4 min wait after removal of the applied field at T^* is slightly greater than that which occurs during a ZFW taken at the normal rate. The step would disappear if the ZFW were taken more slowly.

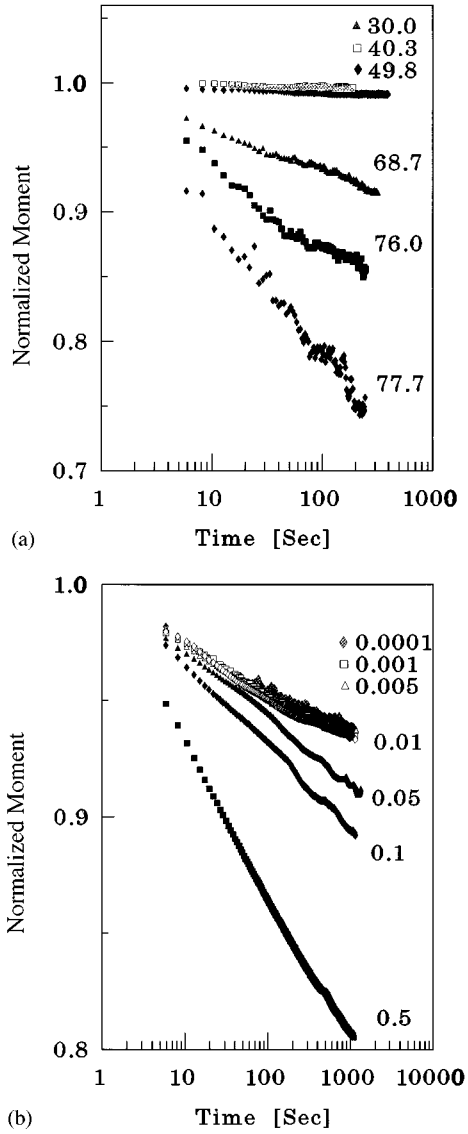

FIG. 10. Magnetic moment plotted against time during a flux creep following removal of the applied field H at temperature T^*. (a) Sample MRB: creep at various temperatures T^* for $\mu_0 H = 10$ μT. (b) Sample BLA: creep for various fields $\mu_0 H$ at $T^* = 69.8$ K. The very large initial slew rate does not allow the response to be followed for the first 1 or 2 sec, but the zero of time is still taken from switch-off with an accuracy of ± 1 sec. The decay is always observed to be logarithmic in time. All moments are normalized to the value obtained by extrapolation to the value at $t = 1$ sec.

or may not be in superconducting contact. If they are indeed in superconducting contact, then each clump can be treated as a more or less spherical piece of granular superconductor. The penetration of a magnetic field into such a superconductor can be characterized by an effective penetration depth, which is given roughly by

$$\frac{\lambda_{\mathrm{eff}}^2}{a^2} = \frac{\phi_0}{2\pi\mu_0(1-f)I_0 a} \approx \frac{1}{(1-f)\beta}, \tag{4.1}$$

where a is the linear spacing between the intergranular contacts, I_0 is the critical current associated with each contact, f is an effective filling factor for the granular material, and

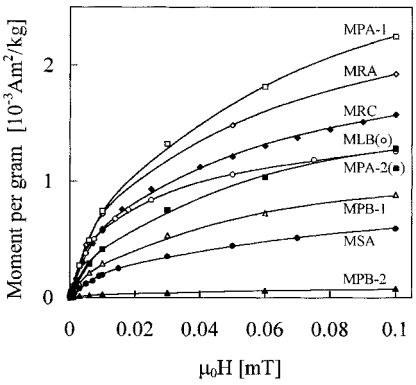

FIG. 11. ZFW magnetic moments per gram at 10 K plotted against applied field for various samples. The solid lines are fits to the double-tanh function described in the text.

β is the McCumber parameter $(2\pi LI_0/\phi_0)$ for a superconducting loop of radius a (inductance L) containing a junction with critical current I_0.[1] The observed diamagnetic fraction in our samples is not apparently related to the clump size, so that the penetration depth $\lambda_{\rm eff}$ must be either much larger than or much smaller than a typical clump size. (The observed reversibility rules out the formation of intergranular flux lines.) If it is much smaller, the intergranular currents in each spherical clump would lead to complete screening of the field, which would lead to a diamagnetic fraction of about $3/(2p)$, where p is the packing fraction within a clump (typically 0.2). Such a diamagnetic fraction is much larger than is observed. We conclude therefore that $\lambda_{\rm eff}$ is much larger than the diameter of the largest clump (about 100 μm). The corresponding intergranular critical current must therefore be very small (the McCumber parameter being less than 0.01), and it is likely to have a negligible effect. We must examine therefore whether the observed diamagnetic fractions can be explained in terms of the behavior of the individual platelets.

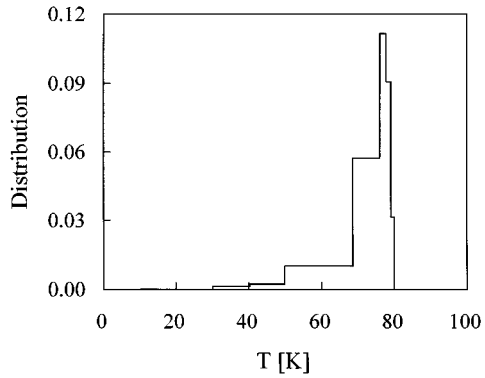

FIG. 12. Distribution function for the temperature at which the local moments become trapped on cooling in an applied field (sample MRB). The function has been obtained from the data shown in Fig. 9 as follows. The difference between the $T=10$ K values of the moment corresponding to field switch-off temperatures of T^* and $T^*+\Delta T^*$ are used to form a histogram against T^*. The values are normalized so that the area under the whole distribution is unity. The distribution shown relates to a cooling field of 10 μT. The distribution is slightly broader for a cooling field of 100 μT.

Let us assume that magnetic interactions between platelets can be neglected. We model each platelet as a spheroid of diameter and thickness equal to that of a typical platelet. We model the random orientation by taking one-third of the platelets to be normal to the applied field, the other two-thirds being parallel to the field. We take the penetration depth for current flow in the ab planes to be 180 nm at low temperatures, the penetration depth for current flow normal to these planes being much larger. The thickness of the platelets being only about 200 nm, the moments produced in platelets parallel to the field will be small and can be neglected. The moment for a platelet normal to the field is obtained by solving numerically the London equation $\nabla^2\mathbf{A}=\mathbf{A}/\lambda^2$, by a method very similar to that described in Ref. 35. The resulting diamagnetic fraction for the random assembly, as defined in Sec. III, is then predicted to be approximately 0.65, somewhat larger than the observed values.

This calculation ignores magnetic interactions between the platelets. We can take crude account of these interactions by using a local mean-field theory. Taking the local field as a third of the magnetization per unit volume and taking into account the observed packing fractions of about 0.2, we find that the necessary correction reduces the diamagnetic fraction by only a few percent.

The value of the penetration depth equal to 180 nm relates to Bi-Sr-Ca-Cu-O that is slightly overdoped with oxygen.[36] Loss of oxygen leads to penetration depths that are significantly larger,[37] values as high as 260 nm having been reported,[38] and to an increase in T_c.[5,39] An increase in penetration depth of this magnitude would be more than enough to account for our observed diamagnetic fractions. Furthermore, we observe some decrease in the diamagnetic fraction after the specimens have been subjected to thermal cycling or mechanical damage. Such cycling is likely to lead to oxygen loss, evidence in our case coming from the observed change in T_c. It is significant that, when a sample whose diamagnetic fraction had been reduced from 0.3 to 0.1 by thermal cycling (MPA-3) was reannealed in oxygen for 72 h at 580 °C, the diamagnetic fraction recovered to 0.53 at 30 K, quite close to the predicted value. We note that this annealing also served to increase the PME component.

We conclude that the observed diamagnetic fractions associated with the moment $M_{\rm FW}$ at low temperatures and low fields can be satisfactorily explained by diamagnetic screening within each platelet, the platelets not being in superconducting contact with each other.

B. Flux line trapping

Our conclusion that the platelets are not in superconducting contact rules out the possibility of intergranular flux trapping.

The extent to which flux lines are trapped *within* a platelet depends on the form of the H-T phase diagram for the platelet, especially near T_c, and on the activation energy required to overcome any barriers opposing the motion of a flux line through the platelet. The associated problems are quite complicated, depending as they do on the shape and size of the platelet and on the fact that a flux line in Bi-Sr-Ca-Cu-O is probably decomposed into pancake vortices at high temperatures. We shall not discuss them here, but we plan to address

them in a future paper. For the present we shall make use of only one theoretical prediction. Suppose that a magnetic field H is applied normally to a flat circular type-II superconducting disk of radius R. The state of minimum Ginsburg-Landau free energy of such a disk contains no flux lines if

$$H<H_{\phi}\approx\frac{\phi_0}{\mu_0 R^2}. \tag{4.2}$$

For platelets of the size relevant to the present experiments and for magnetic fields applied normal to the platelet, the critical field $\mu_0 H_{\phi}$ is roughly 0.5 mT. For a field applied parallel to the platelet, the critical field would be much larger.

We note that the field H_{ϕ} is close in magnitude to the observed field H_v, above which there is a sharp rise in M_{ZFW} (Figs. 3 and 7). We suggest therefore that this rise marks the onset of conventional flux trapping within the platelets. For $B<B_v$, M_{ZFW} must then be due almost entirely to the PME. Conventional flux trapping and the PME seem therefore to be separate and independent effects.

Further evidence in favor of our suggestion comes from several other experiments. We see in Fig. 8 that the field-warm and field-cool curves for the heavily crushed sample MPB-3 coincide within experimental error for fields less than 0.5 mT, but that they diverge at higher fields. This behavior is consistent with the destruction of the PME by crushing and with the retention of flux trapping for $B>B_v\approx 0.5$ mT, confirming that the PME and flux trapping are independent. Very similar behavior was observed in our 2223 powder, which showed little or no evidence of the PME. The moments M_{FC} and M_{FW} coincided within 3% at fields below 0.3 mT and diverged increasingly above that field. Earlier work[40] on Y-Ba-Cu-O powder with similar particle size, and exhibiting no PME, had indicated similar flux trapping behavior, including the dependence (3.2) with $\alpha=1.6$.

It follows from Eq. (3.1) that, at low temperatures and low fields, M_{FC} is due to a linear superposition of the diamagnetic screening moment M_{FW} and the PME moment M_{ZFW}. At higher temperatures, as we saw in Sec. III, M_{FW} in a small field can no longer be due entirely to a diamagnetic screening current, and we conclude therefore that there must then be a contribution from the PME. Nevertheless, Eq. (3.1) is still found to hold. We shall find that the model described in the next section provides a simple explanation of this fact.

In analyzing the bulk of our experimental data in terms of the local moment model, we shall confine our attention to fields up to about $0.2B_v$. We take M_{ZFW} as being due to the PME, with a small correction for trapped flux given by an extrapolation of Eq. (3.2) to low fields.

C. Origin of the paramagnetic Meissner effect: A phenomenological local moment model

We see from Fig. 3 that as a function of the field H in which the sample is cooled the moment that we associate with the PME first rises linearly and then saturates to a constant value.

This dependence of the paramagnetic Meissner moment on the field H suggests strongly that its origin is as follows. Within the sample there are ''entities'' that acquire permanent magnetic moments m when the sample is cooled through the superconducting transition temperature. These *local moments* are like the atomic moments in a conventional paramagnetic material, although their spatial extent may be greater. Furthermore, unlike atomic moments, the moments m may have magnitudes that depend on temperature; for example, they may increase with decreasing temperature below T_c, and they may not set in until the temperature has fallen to some value that is significantly less than T_c. If the cooling takes place in zero applied magnetic field, the moments are oriented at random and give rise to no net paramagnetic moment. If cooling takes place in a field H, a finite net moment will be established, as in a conventional paramagnetic material. If interactions between the local moments can be neglected and if the system is in thermal equilibrium, the net moment will be given by an appropriate Brillouin function. In the simple case where each local moment can point in only two directions (parallel or antiparallel to the field), the total moment will be given by

$$M=Nm\tanh\left(\frac{\mu_0 mH}{k_B T}\right), \tag{4.3}$$

where N is the total number of local moments in the sample.

The fact that a paramagnetic Meissner moment remains in place after the polarizing magnetic field has been removed (The ZFW line in Fig. 2) shows that nonequilibrium moments can be frozen in. This means that the reorientation of a local moment must involve the surmounting of a potential barrier. Let the magnitude of this barrier be U_0 in the absence of an applied field. The rate at which the barrier can be surmounted in zero field is then given by

$$\nu=\nu_0\exp\left(-\frac{U_0}{k_B T}\right), \tag{4.4}$$

where ν_0 is an attack frequency. Moments will be frozen in if $1/\nu>t_0$, where t_0 is the time scale over which an experiment is conducted; i.e., they will be frozen in if

$$T<T_f=\frac{U_0}{k_B\ln(\nu_0 t_0)}. \tag{4.5}$$

We have assumed that the barrier U_0 is not affected much by the small applied field. Equation (4.3) then holds only for $T>T_f$; if $T<T_f$,

$$M=Nm\tanh\left(\frac{\mu_0 mH(T_f)}{k_B T_f}\right), \tag{4.6}$$

where $H(T_f)$ is the field to which the system was exposed during cooling through the temperature T_f. Of course, the transition between Eqs. (4.3) and (4.6) will not be abrupt at $T=T_f$, although the rapid variation of ν with T [Eq. (4.4)] will ensure that the transition is quite rapid. Strictly speaking, Eq. (4.6) will hold only at a temperature just below T_f. Later, we shall apply the equation [or its generalization (4.7)] at temperatures well below T_f. This procedure will fail to take account of the fact that the local moment m is temperature dependent. This temperature dependence is responsible for the fact that curves such as FG in Fig. 2 rise with decreasing temperature; examples of this rise in real

data are shown in Fig. 9. The value of m inside the tanh should be the moment at a temperature just below T_f, while the value of m outside the tanh should be the moment at the low temperature. However, as we see from Fig. 9, these moments differ by only about 30%, which is probably less than other uncertainties that are present in our analysis.

In practice, different local moments may have associated with them different values of m and T_f. Equation (4.6) must then be generalized to

$$M=\sum_i N_i m_i \tanh\left(\frac{\mu_0 m_i H(T_{fi})}{k_B T_{fi}}\right). \tag{4.7}$$

If the moments can point in any direction, these results will be modified, but only to a minor quantitative extent.

In this analysis we have ignored magnetic interactions between adjacent local moments. We shall argue later that this neglect is justified.

D. Comparison of the local moment model with experiment

We show now that the phenomenological local moment model can give a satisfactory description of the observed paramagnetic Meissner effect, provided that the local moments are assumed to have certain characteristics.

At temperatures above T_p the magnitudes of the local moments must be negligible. As the sample is cooled below T_p in a field H ($T_p \rightarrow E \rightarrow C$), the moments become significant and are partially or totally aligned by the field. At a sufficiently low temperature, the moments become frozen in, and there is no reorientation when the field is removed. But the field removal eliminates the diamagnetic screening currents. The moment M_{ZFW} must then be due simply to the frozen-in moments (i.e., the PME), and Eq. (3.1) must obviously be obeyed.

As we have already noted, the FC curve ($T_c \rightarrow E \rightarrow C$ in Fig. 2), is reversible only if traversed sufficiently slowly. This is consistent with the idea that reorientation of the local moments takes time. We also noted that if the field is turned off at a point E, say, the net paramagnetic moment increases abruptly, corresponding to an abrupt loss of the diamagnetic screening moment, and then relaxes back by some 10–20 % in such a way that the change in moment is proportional to the logarithm of the time [Figs. 10(a) and 10(b)]. We identify this relaxation with a gradual reorientation of the local moments that have not been completely frozen in at the temperature concerned. As can easily be shown analytically and has been shown by computer modeling,[28] the logarithmic dependence on time can be accounted for if there is a wide spread of relaxation rates ν as defined in Eq. (4.4). We identify the curve $F \rightarrow G$, taken after relaxation at the temperature T^*, as being due to a temperature dependence of the magnitudes of the local moments m_i rather than in the *number* of moments that are frozen in. Below about 50 K there is little relaxation, the $F \rightarrow G$ and the ZFW curves almost coincide, and all temperature dependences must be associated with temperature dependences of the m_i's.

In reality, there may be a range of freezing-in temperatures T_f. Our measurements allow us to judge the width of this range. We have followed curves of the type $F \rightarrow G$ for a range of temperatures T^*, and we have measured the moments $M(T^*)$ to which these curves tend at the lowest temperature. The moment $M(T^*)$ is due to those moments with energy barriers high enough to ensure freezing-in at the temperature T^*. If we assume that at the relevant temperatures all the moments m_i have the same magnitude, we can deduce distribution functions such as those shown in Fig. 12. We can see that it is sharply peaked at a temperature of about 77 K. In our later analysis we shall therefore take T_{fi} to be constant and equal to 77 K.

We have already noted that the moment along the FW line ($B \rightarrow T_c$ in Fig. 3) is due to diamagnetic screening at temperatures below about 50 K, but that a component due to the PME must be present at higher temperatures, with Eq. (3.1) still holding. This is easily understood. Below about 50 K there can be no reorientation of the local moments, and therefore they can make no contribution to M_{FW} after a zero-field cool. Above about 50 K some of the local moments can change their orientations within the time scale of an experiment, and these moments will contribute to M_{FW}. At a given temperature it is these same moments that are subject to relaxation following field removal at the point E during a field cool. Thus, at temperatures exceeding about 50 K, Eq. (3.1) still holds at the low fields of interest here (see Fig. 4), the contribution to M_{FW} from the local moments being equal to the difference between the contributions of these moments to M_{FC} and M_{ZFW}. (It is interesting to note that this type of behavior would be different if the PME that is established during a field cool were due to a nonequilibrium distribution of flux trapped during cooling through T_c.)

If, as we suggest, the form of the curve AD in Fig. 2 can, in the absence of flux trapping, be described by a superposition of Brillouin functions, such as is given by Eq. (4.7), then we ought to be able to use this curve to obtain information about the number and magnitude of the local moments present in our samples. Although the expression (4.6) gives a *qualitatively* correct description of our results, it is not in *quantitative* agreement with the observed dependence of the moment M_{ZFW} at a low temperature on the field H in which cooling takes place, as we see from Fig. 7. We are led therefore to try the more general expression (4.7). As we have just seen, there is evidence that T_{fi} can be taken as constant and equal to 77 K, so that we must assume that the localized moments M_i are spread over a range of values. In fact, for all our samples, we can fit our experimental results by assuming that there are just two groups of localized moments: a total of N_1 entities each with magnetic moment m_1 and N_2 entities each with moment m_2, both with $T_f = 77$ K. In carrying out this fitting procedure, we have included data at fields in which there is some conventional flux trapping, and we have assumed that this trapping is correctly described by an equation of the form (3.2), the parameters a and α being determined from fits at high field, where the PME makes a negligible contribution. Examples of the quality of the fit are shown in Figs. 7 and 11. Of course, the assumption that there are only two groups of moments is likely to be an oversimplification, but the values m_1, m_2, N_1, and N_2 are likely nevertheless to represent a *valuable estimate of the magnitudes of the local moments and their concentrations and of the spread of these values*. We find that most of the moments have a value of about 4×10^{-17} A m^{-2} at a concentration of typically 2×10^{13} kg^{-1} (equivalent to a concentration per

unit volume of sample of typically 3×10^{16} m^{-3}, which is a factor of about 10 less than the concentration of platelets), but that a few percent of the moments are a factor of order 10 larger.

The analysis that we have carried out in this section has been based on two assumptions relating to the neglect of magnetic interactions: first, between the local moments themselves and, second, between the local moments and the diamagnetic moments of the surrounding diamagnetic particles. We can judge whether the first is a reasonable assumption by incorporating a Lorentz local magnetic field in the deviation of the total magnetic moment of the assembly of local moments. If all the moments have the same value m, at a concentration N/V per unit volume of sample, the effect of the Lorentz field is to introduce a Curie temperature, given by

$$T_{\text{Curie}}=\frac{\mu_0 m^2 N}{3k_B V}. \tag{4.8}$$

Using the values $m=3\times10^{-16}$ A m^2 and $N/V=1.3\times10^{15}$ m^{-3}, appropriate to the small concentration of large moments, which will have the highest Curie temperature, we find that $T_{\text{Curie}}\approx4$ K. It follows that the interactions will have only a small effect at temperatures of order 70 K, where freezing in of the moments occurs.

Turning now to the second type of magnetic interaction, we see that during a field cool the local moments responsible for the PME are exposed to a combination of the external field and the field due to the diamagnetic moments of the surrounding particles. The effect of the surrounding particles can be viewed as a local field, and as we have already seen in Sec. IV B, the effect of this local field is quite small and can be neglected.

We find that both thermal cycling and mechanical damage result in a substantial reduction in the PME and that this reduction is due generally to a reduction in the *concentration* of local moments rather than in their magnitudes, the reduction in the concentration of large moments being particularly strong. An exception is provided by the heavy compression of the powder, which results in a reduction in both moment magnitude and moment concentration. As we mentioned in Sec. IV B, annealing in oxygen of a powder sample serves to reverse the loss of the PME moment due to thermal cycling.

E. Origin of the local moments

Our model supposes that there are within some of the superconducting particles entities that have permanent magnetic moments, due presumably to persistent circulating currents, even in the absence of an applied magnetic field and in the absence of conventional flux trapping. Such moments can appear only if there is breaking of time-reversal symmetry.

It has been suggested[4,23,26] that the paramagnetic Meissner effect is due to superconducting loops that contain one or more Josephson junctions, an odd number of such junctions within a loop having a negative coupling energy. Such a loop breaks time-reversal symmetry. Consider a circular loop, radius R, containing one such junction. Its inductance L is roughly $\mu_0 R$. If the McCumber parameter $\beta=2\pi LI_0/\phi_0$ is significantly greater than unity and the applied field is zero, the states with minimum energy contain trapped flux equal to, or a little less than $\pm\phi_0/2$ and have magnetic moments given approximately by

$$m=\pm\frac{\pi R\phi_0}{2\mu_0}. \tag{4.9}$$

Transitions between these two values are opposed by a potential barrier.

In principle, such loops could provide the localized moments with which we are concerned. They might be formed from rings of platelets, the junctions being formed at the points of contact between the platelets, although there is evidence, as we have seen, that *generally* these contacts are not superconducting. Mechanical damage might well destroy such loops, so that the observed effect of such damage in destroying the moments would receive a natural explanation. However, for the typical powdered material on which we have carried out experiments, such loops will presumably have radii of order the width of a platelet in the ab plane, i.e., of order 1 μm. Equation (4.9) then leads to a moment of order 2.6×10^{-15} A m^2, which is a factor of almost 100 larger than the majority of the observed moments. In fact, to obtain from Eq. (4.9) a moment as small as the majority of those observed, it would be necessary to take R less than a penetration depth, which is fundamentally impossible. A single π junction *sharing two loops* could have an arbitrarily small magnetic moment if the loops are of essentially the same size. However, such a geometry seems very unlikely to arise in a random arrangement of grains. We conclude that intergranular loops containing a π junction are unlikely to be responsible for the PME.

This conclusion can be strengthened by the following argument. To obtain the required value for the local moment, the loop size would certainly have to be comparable with the penetration depth. This would require a circulating current in each loop of order 5 mA in order to generate half a flux quantum. We might try to imagine such a loop to be formed from several platelets in contact, the π junction forming at a point of contact between two platelets; if, as we have already estimated, the area of contact between two platelets is about 0.2 μm^2, the current density through the junction would have to be greater than 10^{11} A m^{-2}, which is larger than the critical current in a single Bi-Sr-Ca-Cu-O crystal at low temperatures (typically 10^8 A m^{-2}) (Ref. 41), and is therefore quite unreasonably large.

Another possibility is that a loop forms within a platelet, the junctions existing at grain boundaries. One interesting and attractive possibility is that the loop is centered on the intersection of three grain boundaries, the effective π junction forming between differently oriented crystals and being associated with d-state pairing in the superconductor.[24,25] Yet another possibility is that a platelet contains one grain boundary with a negative Josephson coupling energy along *part* of its length.[42] However, confinement of the trapped flux within an area comparable with the square of the penetration depth would again require currents through the grain boundaries that are unrealistically large.

In fact, there is a more serious objection to these possibilities. The required half-quantum flux trapping would amount to the trapping of something like a half-quantum flux

line. At first sight the moment associated with such a flux line is $(\phi_0 t/2\mu_0)$, where t is the thickness of the platelet and where we have taken account of only the circulating current flowing within a penetration depth of the core of the vortex. However, such a calculation ignores the current that must necessarily flow on the whole surface of the platelet, to a depth equal to the penetration depth, associated with the return flux. This latter contribution is particularly important in the case where t is small; in our platelets, t is not much larger than the relevant penetration depth. Taking account of this extra current, we estimate that the moment is probably increased by an amount equal to roughly $(\phi_0 R/2\mu_0)$, where R is the radius of the platelet. [A general expression for the moment of a platelet containing a flux line at its center seems not to be available. We have therefore based our estimate on published calculations of the current distribution due to one flux line in an infinite disk of thickness t, in two limits. In the case $t \ll \lambda$,[43] the current is uniformly distributed across the thickness of the disk and falls off as $(1/r^2)$ at distances large compared with an effective penetration depth of $2\lambda^2/t$. In the case $t \gg \lambda$,[44] the current in the bulk is significant only out to a distance of order λ, but there is in addition a surface current density that again falls off as $(1/r^2)$, at distances large compared with the ordinary penetration depth λ. For a disk of finite radius R, large compared with the relevant penetration depth, with one conventional flux line at its center, the surface current in both limits contributes an amount $(\phi_0 R/\mu_0)$ to the total magnetic moment. In the case $t \gg \lambda$, there is an additional contribution equal to $(\phi_0 t/\mu_0)$ from the current flowing in the bulk. Our estimate of the moment in the case when $t \approx \lambda$ is based on the reasonable assumption that the surface contribution $(\phi_0 R/\mu_0)$ is present throughout the transition between the two extreme limits.] This increased moment is certainly very much larger than that observed, so that *intragranular* loops, including those that might be associated with d-state pairing in a tricrystal, seem also to be ruled out. This conclusion is of course based on the assumption that the half-quantum flux line round which the loop forms is on average not too far from the center of a platelet. If the flux line were always positioned very close to the edge of a platelet, then the moment could be reduced to a value comparable with that observed.

Yet another possibility is that the local moments arise from the fundamental nature of the superconductivity in Bi-Sr-Ca-Cu-O. If the superconducting ground state lacks time-reversal symmetry, the ground state of an individual crystal can in principle carry a circulating current and therefore have a magnetic moment. A search for such moments in Y-Ba-Cu-O powder was unsuccessful.[40] If, as has been suggested, the pairing in Y-Ba-Cu-O is $d_{x^2-y^2}$, time-reversal symmetry is not violated, and no moment would be expected. The situation might be different in Bi-Sr-Ca-Cu-O. However, we must emphasize that our results suggest that only a small fraction (of order 1 in 10) of the platelet crystals in our Bi-Sr-Ca-Cu-O samples exhibit a moment, so that evidence for any general violation of time-reversal symmetry is lacking. Perhaps the pairing is modified in a small fraction of the Bi-Sr-Ca-Cu-O crystals, as a result, for example, of strain. Again, mechanical damage might then lead to loss of the moments, although it is curious that the less extreme forms of mechanical damage seem to reduce the *number* of local moments without affecting the magnitudes of those that remain. Yet another possibility is related to the fact that any circulating current arising from a violation of time-reversal symmetry is confined to the surface of the sample and that its magnitude is strongly affected by the boundary conditions on the order parameter at the sample surface.[45] Any moment arising from a surface current could therefore be affected strongly by local oxygen loss from the surface of a platelet. As we have seen in Sec. IV B, there is some evidence that mechanical damage can lead to oxygen loss, so that the loss of the PME in some of the platelets following mechanical damage could indeed be associated with oxygen loss from their surfaces. Further experiments would be required before firm conclusions could be drawn.

F. Bulk samples and analyses by other authors

We have analyzed the data for a bulk ceramic sample in the same way as for the powder samples. Again, we take the ZFW data and obtain the PME component by subtracting a component due to conventional trapped flux that is assumed to be given by an expression of the form (3.2), the parameters a and α being determined from the observed behavior at high magnetic fields. The component due to conventional trapped flux is much larger than is the case with powdered samples, and so the procedure by which the PME is extracted is less reliable. To the extent that our procedure is formally equivalent to a fitting of the FC data to the sum of a trapped field term, a conventional Meissner moment, and a term due to the PME, we are following other authors. We find that the values of the localized moments derived from the double-tanh fit are very similar to those obtained from the powder samples, a fact that adds support to our view that the PME is *not* associated with intergranular contacts.

As we mentioned in the Introduction, other authors have analyzed their experimentally observed FC curves in terms of Eq. (1.1), where the first term on the right-hand side incorporates the effects of diamagnetic flux expulsion and of flux trapping, while the second term describes the fundamental paramagnetic Meissner effect. This second term incorporates a field H_0 describing the interactions between the moments responsible for the paramagnetic Meissner effect.

We emphasize that in our own analysis we have assumed that interactions between the local moments can be neglected, and we have presented evidence in favor of this assumption. In contrast, the formula (1.1) and the orbital glass model underlying it are based on the idea that there are strong interactions between the local moments. We mention at this point one other piece of evidence that interactions are not important. We have obtained values of M_0 and H_0 by fitting Eq. (1.1), for three representative groups of samples (powder, sintered material, and ground sintered material), some of which were used in our own work and some in the work of others. We find that within any given group H_0 decreases with increasing M_0. This is contrary to expectation if H_0 is to be associated with interactions.

We have reanalyzed the experimental results of other authors in terms of our own model, in the same way as for our own bulk samples. We find that the magnitudes of the result-

ing local moments and their concentrations turn out to be very similar to those found for our own samples, if we use a single-tanh function. This points strongly to a common origin for the moments found in all samples, and it further reinforces our view that the PME is not associated with intergranular contacts.

We recall from Sec. I that some authors[23,26] have used relation (1.2) to deduce an effective loop area S associated with each local moment. Typically, S has a magnitude of a few square micrometers, which could arise only if the loops are formed from a number of grains. Equations of the form (1.2) are based on simple and unrealistic models. In our approach the crossover field H_{c0} results from a balance between the PME on the one hand and conventional diamagnetism and flux trapping on the other; these two groups of phenomena being, as we see it, unrelated, there is no basis for Eq. (1.2). Indeed, the application of Eq. (1.2) to a set of our own samples, derived by successive crushing of a bulk ceramic sample, gives rise to a value of S that increases as the clump size decreases and indeed becomes larger than the clump size for the most severely crushed powder. This does not make sense. We suggest that the use of Eq. (1.2) is not justified.

V. CONCLUSIONS

We have presented experimental results on the paramagnetic Meissner effect, and we have concentrated our attention on the effect as observed in finely powdered Bi-Sr-Ca-Cu-O produced by spray pyrolosis. We have presented arguments, based on the form of the experimental data, for supposing that the PME is not due to conventionally trapped flux lines, and we have described how these arguments lead to a procedure for separating the effects due to the PME from those due to trapped flux. These arguments are not rigorous, but we have taken the view that they are sufficiently good to make it worthwhile pursuing an analysis based on them. In this analysis we have introduced a *local moment model* in which the PME arises from the presence within the powders of local magnetic moments of unspecified nature, which form just below the superconducting transition temperature. At high temperatures the moments can be partially oriented by an applied magnetic field and therefore contribute to a net moment, but the net moment becomes frozen in at a lower temperature. Our experimental results are broadly consistent with this model, and we are able to deduce the magnitudes of the moments, their concentrations, and the temperatures at which freezing-in occurs. The suggestion that the moments arise from superconducting loops containing an odd number of Josephson junctions with negative coupling energy is examined, but it is shown that the magnitudes of the moments, as deduced from our analysis, are almost certainly too small to be consistent with this suggestion. Another possibility is that the effect is associated with some fundamental violation of time-reversal symmetry within the single-crystal grains, although, if our analysis is correct, the effect must be confined to only a small fraction of the grains. A possible conclusion of our work is that the local moment model is in fact incorrect and that the PME is due to some form of more or less conventional flux trapping, taking place in addition to, and independently of, that described by Eq. (3.2). The possibility that forms of conventional flux trapping are indeed responsible for the PME has been suggested in several recent papers.[15–17] However, a theory of such flux trapping, relevant to the PME in very small particles and consistent with our observations, has yet to be developed.

ACKNOWLEDGMENT

We are grateful to Dr. G. F. Cox for help with the calculations on diamagnetic fractions.

*On leave from Cryogenic Laboratory, Chinese Academy of Sciences, P.O. Box 2711, Beijing 100080, P. R. China.

[1] J. R. Clem, Physica C **153-155**, 50 (1988).
[2] P. Svedlindh, K. Niskanen, P. Norling, P. Nordblad, L. Lundgren, B. Lönnberg, and T. Lundström, Physica C **162-164**, 1365 (1989).
[3] F. J. Blunt, A. R. Perry, A. M. Campbell, and R. S. Liu, Physica C **175**, 539 (1991).
[4] W. Braunisch, N. Knauf, V. Kataev, S. Neuhausen, A. Grütz, A. Kock, B. Roden, D. Khomskii, and D. Wohlleben, Phys. Rev. Lett. **68**, 1908 (1992).
[5] W. Braunisch, N. Knauf, G. Bauer, A. Kock, A. Becker, B. Freitag, A. Grütz, V. Kataev, S. Neuhausen, B. Roden, D. Khomskii, and D. Wohlleben, Phys. Rev. B **48**, 4030 (1993).
[6] B. Schliepe, M. Stindtmann, I. Nikolic, and K. Baberschke, Phys. Rev. B **47**, 8331 (1993).
[7] V. Kataev, N. Knauf, W. Braunisch, R. Müller, R. Borowski, B. Roden, and D. Khomskii, Pis'ma Zh. Éksp. Teor. Fiz. **58**, 656 (1993) [JETP Lett. **58**, 636 (1993)].
[8] K. Niskanen, J. Magnusson, P. Nordblad, P. Svedlindh, A-S. Ullström, and T. Lundström, Physica B **194-196**, 1549 (1994).
[9] S. Thöming, J. Kötzler, M. W. Pieper, and A. Spirgatis, Verh. Dtsch. Phys. Ges. VI **27**, 912 (1992).
[10] N. Knauf, W. Braunisch, G. Bauer, A. Kock, A. Becker, B. Freitag, V. Kataev, B. Roden, and D. Khomskii, Physica B **194-196**, 2229 (1994).
[11] W. H. Lee, Y. T. Huang, S. W. Lu, K. Chen, and P. T. Wu, Solid State Commun. **74**, 97 (1990).
[12] M. D. Lan, J. Z. Liu, and R. N. Shelton, Phys. Rev. B **43**, 12 989 (1991).
[13] S. Riedling, G. Bräuchle, R. Lucht, K. Röhberg, H. v. Löhneysen, H. Claus, A. Erb, and G. Müller-Vogt, Phys. Rev. B **49**, 13 283 (1994).
[14] D. J. Thompson, M. S. M. Minhaj, C. E. Wenger, and J. T. Chen, Phys. Rev. Lett. **75**, 529 (1995).
[15] E. Zeldov, A. I. Larkin, V. B. Geshkenbein, M. Konczykowski, D. Majer, B. Khaykovich, V. M. Vinokur, and H. Shtrikman, Phys. Rev. Lett. **73**, 1428 (1994).
[16] A. E. Koshelev and A. I. Larkin, Phys. Rev. B **52**, 13 559 (1995).
[17] P. Kostic *et al.*, Phys. Rev. B **53**, 791 (1996).
[18] L. N. Bulaevskii, V. V. Kuzii, and A. A. Sobyanin, Pis'ma Zh. Éksp. Teor. Fiz. **25**, 314 (1977) [JETP Lett. **25**, 290 (1977)].
[19] V. B. Geshkenbein and A. I. Larkin, Pis'ma Zh. Éksp. Teor. Fiz. **43**, 306 (1986) [JETP Lett. **43**, 395 (1993)].
[20] V. B. Geshkenbein, A. I. Larkin, and A. Barone, Phys. Rev. B **36**, 235 (1987).
[21] L. N. Bulaevskii, V. V. Kuzii, and A. A. Sobyanin, Solid State Commun. **25**, 1053 (1978).

[22] B. I. Spivak and S. A. Kivelson, Phys. Rev. B **43**, 3740 (1991).
[23] M. Sigrist and T. M. Rice, J. Phys. Soc. Jpn. **61**, 4283 (1992); J. Low Temp. Phys. **95**, 389 (1994).
[24] D. A. Wollman, D. J. Van Harlingen, W. C. Lee, D. M. Ginsberg, and A. J. Leggett, Phys. Rev. Lett. **71**, 2134 (1993).
[25] A. Mathai, Y. Gim, R. C. Black, A. Amar, and F. Wellstood, Phys. Rev. Lett. **74**, 4523 (1995).
[26] F. V. Kusmartsev, Phys. Rev. Lett. **69**, 2268 (1992).
[27] F. V. Kusmartsev, Phys. Lett. A **169**, 108 (1992).
[28] J. Magnusson, J-O. Andersson, M. Björnander, P. Nordblad, and P. Svedlindh, Phys. Rev. B **51**, 12 776 (1995).
[29] D. Dominguez, E. A. Jagla, and C. A. Balseiro, Phys. Rev. Lett. **72**, 2773 (1994).
[30] C. Auletta, G. Raiconi, R. De Luca, and S. Pace, Phys. Rev. B **51**, 12 844 (1995).
[31] S. V. Bhat, A. Rastogi, N. Kumar, R. Nagarajan, and C. N. R. Rao, Physica C **219**, 87 (1994).
[32] Ch. Heinzel, Th. Theilig, and P. Ziemann, Phys. Rev. B **48**, 3445 (1993).
[33] D. Khomskii, J. Low Temp. Phys. **95**, 205 (1994); Physica C **235**, 293 (1994).
[34] T. J. Jackson, M. N. Keene, and C. E. Gough, Meas. Sci. Technol. **3**, 988 (1992).
[35] E. M. Parvin, A. Singfield, W. F. Vinen, and G. F. Cox, Supercond. Sci. Technol. **6**, 525 (1993).
[36] S. L. Lee, P. Zimmermann, H. Keller, M. Warden, I. M. Savic, R. Schauwecker, D. Zech, R. Cubitt, E. M. Forgan, P. H. Kes, T. W. Li, A. A. Menovsky, and Z. Tarnawski, Phys. Rev. Lett. **71**, 3862 (1993).
[37] Y. J. Uemura, G. M. Luke, B. J. Sternlieb, J. H. Brewer, J. F. Carolan, W. N. Hardy, R. Kadono, J. R. Kempton, R. F. Kiefl, S. R. Kreitzman, P. Mulhern, T. M. Riseman, D. Ll. Williams, B. X. Yang, S. Uchida, H. Takagi, J. Gopalakrishnan, A. W. Sleight, M. A. Subramanian, C. L. Chien, M. Z. Cieplak, Gang Xiao, V. Y. Lee, B. W. Statt, C. E. Stronach, W. J. Kossler, and X. H. Yu, Phys. Rev. Lett. **62**, 2317 (1989).
[38] A. Maeda, Y. Lino, T. Hanaguri, N. Motohira, T. Kishio, and T. Fukase, Phys. Rev. Lett. **74**, 1202 (1995).
[39] C. Allgeier and J. S. Schilling, Physica C **168**, 499 (1990).
[40] T. J. Jackson, M. N. Keene, W. F. Vinen, and P. Gilberd, Physica B **165-166**, 1437 (1990).
[41] See, for example, D. Larbalestier, Phys. Today **44**(6), 74 (1991).
[42] D. X. Chen and A. Hernando, Europhys. Lett. **26**, 365 (1994); Phys. Rev. B **50**, 10 107 (1994).
[43] J. Pearl, Appl. Phys. Lett. **5**, 65 (1964).
[44] M. B. Ketchen, W. J. Gallagher, A. W. Kleinsasser, S. Murphy, and J. R. Clem, in *SQUID85—Superconducting Quantum Interference Devices and their Applications*, edited by H. D. Hahlbohm and H. Lübbig (Walter de Gruyter & Co., Berlin, 1985), p. 865.
[45] M. Sigrist, T. M. Rice, and K. Ueda, Phys. Rev. Lett. **63**, 1727 (1989).